PROCEEDINGS OF SCIENCE

Measurement of (p+He)-induced anisotropy in cosmic rays with ARGO-YBJ

R. Iuppa[*a,b], **S. Cui**[c], **G. Di Sciascio**[a], **S.M. Mari**[d], **P. Montini**[a] **on behalf of the ARGO-YBJ Collaboration**

[a] *INFN, Sezione Roma Tor Vergata, Roma,* roberto.iuppa@roma2.infn.it
[b] *Dipartimento di Fisica dell'Università di Roma Tor Vergata, Roma, Italy*
[c] *Hebei Normal University, Hebei, P.R. China*
[d] *Dipartimento di Fisica dell'Università Roma Tre and INFN , Sezione Roma Tre, Roma, Italy*

Deviations from isotropy in the cosmic ray arrival direction distribution indicate the laboratory reference frame moving with respect to the cosmic radiation. When data are ordered in sidereal time, any effect is of great importance, as it may trace potential sources of cosmic rays and probe their propagation through magnetic fields. For the same reason, to decipher results implies unfolding effects from source distribution, energy spectrum and mass composition of cosmic rays, as well as magnetic field on regular and turbulent scales. Any efficient selection of cosmic ray mass would have a major impact on this scenario, as parameters related to cosmic rays production site, acceleration and propagation mechanisms would be importantly constrained in terms of rigidity. So far, no experiment managed to implement efficient mass selections and save high statistics at the same time. The ARGO-YBJ experiment (located at the YangBaJing Cosmic Ray Observatory, Tibet, China, 4300 m asl) is the only detector able to select the cosmic ray light (p+He) component with high efficiency in the wide energy range few TeV - 10 PeV. In this paper a preliminary analysis of the Galactic CR anisotropy for (p+He)-induced events with the ARGO-YBJ experiment will presented.

The 34th International Cosmic Ray Conference,
30 July- 6 August, 2015
The Hague, The Netherlands

*Speaker.

PoS(ICRC2015)290

1. Introduction

The cosmic ray (CR) arrival direction distribution and its anisotropy has been a long-standing problem ever since the 1930s. In fact, the measurement of the anisotropy is a powerful tool to investigate the propagation mechanisms and the spatial sources distribution.

Data show that the almost perfect isotropy is broken by a dipole-like feature with an amplitude of $\sim 10^{-4}$ - 10^{-3} evolving with the energy (the so-called *"Large-Scale Anisotropy"*, LSA). The existence of two distinct broad anisotropy regions in sidereal time, one showing an excess of CRs (called *"tail-in"*), distributed around 40° to 90° in Right Ascension (R.A.), the other a deficit (the *"loss cone"*), distributed around 150° to 240° in R.A., has been clearly observed by many experiments with increasing sensitivity and details in both hemispheres (for a review see, for example, [1]). The center of the "tail-in" component is close to the direction of the heliospheric tail, which is opposite to the proper motion direction of the solar system. The center of the "loss cone" deficit component points to the direction of the north Galactic pole. These observations rule out the hypothesis that a Compton-Getting effect [2] due to the motion of the heliosphere with respect to the local insterstellar medium (expected as a dipole with a maximum in the direction of the Galactic Center decl.$\simeq$49°, R.A.$\simeq$315° and a larger amplitude 3.5×10^{-3}) is a major source of the anisotropy.

An intriguing result by IceCube [3] is the confirmation of the EAS-TOP finding [4] in the Northern hemisphere, that the anisotropy 'flip' around 100 TeV and its morphology changes. Below about 100 TeV, the global anisotropy is dominated by the dipole and quadrupole components. At higher energies the non-dipolar structure of the anisotropy challenges the current models of CR diffusion. At PeV energies the IceTop experiment showed that anisotropy persists with the same structure as at $\sim$400 TeV, but with a deeper deficit [5]. Whether the strengthening of the deficit region at PeV energies is due to propagation effects from a given source or to the contribution of heavier nuclei at the knee is not clear [6]. As a consequence, the measurement of the anisotropy for each of the CR charge groups individually across the knee should be a high priority of the next generation ground-based experiments in order to discriminate between different propagation models of CRs in the Galaxy.

In this paper a preliminary analysis of the Galactic CR anisotropy for (p+He)-induced events with the ARGO-YBJ experiment is presented. The ARGO-YBJ experiment has been in stable data taking for more than 5 years at the YangBaJing Cosmic Ray Laboratory (Tibet, P.R. China, 4300 m a.s.l., 606 g/cm^2). With a duty-cycle of $\sim$87% the detector collected about $5\cdot10^{11}$ events in a wide energy range, from few hundreds GeV up to 10 PeV.

2. Strategy of analysis

For anisotropy studies, the background is the number of events thatare expected to be collected in case of isotropy. For a given solid angle around a given direction in the sky, such a number is related to the primary flux, the effective area of the selection and the exposure time. Assuming typical time-scales of variation of the primary flux to be much longer than one sidereal day, it allows one to consider the primary flux as practically constant in time. As a consequence, potential variations of the background are only induced by time-space variations of the effective area, which

in turn depends on trigger, selection and reconstruction efficiencies. Estimating background means accounting for all these variations and correcting for their effect on the expected number of isotropically distributed events. Consequently, the significance of the observation directly depends on the extent of validity of the background method underlying assumptions.

In this analysis we used the *"ratio-method"*, using the complete set of events as reference for the estimation of the background of a particular subset of events. The idea is to measure the *local* fraction of *selected* to *all* events, i.e., to divide the sky into many same-size cells and to estimate for each cell the ratio *selected* to *all*. When represented together, the cells will produce the sky-map of the ratio, possibly showing excesses somewhere and defects elsewhere. If necessary corrections are applied to account for different exposures and geometrical acceptances, then the average value of the ratio all over the map, will be the ratio of fluxes *selected/all*[1] and, by construction, any feature found in this sky-map may be interpreted as an excess or a deficit of *selected* events *relative* to the underlying all-particle event anisotropy.

The ratio is an observable less subject to systematic effects than time-averages or equi-zenith symmetrisations , because biases may only come from variations affecting *selected* events in a different way than *all*-particle ones. For all other issues, determining global or local changes in time periods whatever long, everywhere in the sky the *selected* events will exhibit the same variations as the whole set will, leaving unchanged the ratio. A similar feature is benefited by the East-West method , although in this case only projections of the anisotropy along declination belts around the zenith of the experiment could be derived.

In the following we will show how to estimate the ratio of the acceptances of SEL and ALL events using data only. Provided that the first application of the method is to look for anisotropy induced by light elements (p+He) in the cosmic radiation, we will refer to them now instead of SEL, using the subscript ℓ. For the ALL events, no subscript will be used.

2.1 Primary fluxes and number of events

Let the all-particle primary flux be $\phi(\xi,t)$ and let us neglect any dependence on time: $\phi(\xi,t) \rightarrow \phi(\xi)$. Let the all-particle event rate from the direction $\mathbf{x}$ of the sky be $F(\mathbf{x},t)$. It holds

$$F(\mathbf{x},t) = \phi\left(R^{-1}(t)\,\mathbf{x}\right)\, a(\mathbf{x},t)\, e(t)\, \omega$$

where $\mathbf{x} = R(t)\xi$ is the relation between local ($\mathbf{x}$) and equatorial coordinates (ξ), $\phi(\xi)$ is the primary flux, $a\,(\mathbf{x}(\xi,t))$ is the effective area, $e(t)$ is the exposure in the time interval considered and ω is the solid angle. Notice that both ϕ and a depend also on the primary energy spectrum, but this detail is unessential in this context and will not be made explicit.

We will use $\phi\,(\mathbf{x},t)$ to indicate $\phi\left(R^{-1}(t)\,\mathbf{x}\right)$ and often interchange ξ and $(\mathbf{x},t)$. We now assume that dependences of the effective area on direction $\mathbf{x}$ and time t are *separable*: $a(\mathbf{x},t) = g(\mathbf{x})\, r(t)$. In a similar way, the light-particle primary flux and event rate could be introduced, with the following relation holding:

$$F_{tag}(\mathbf{x},t) = \left[\phi_\ell\,(\mathbf{x},t)\; a_{tag}(\mathbf{x},t) + \phi_{\mathrm{non}-\ell}\,(\mathbf{x},t)\; c_{tag}(\mathbf{x},t)\right]\, e(t)\, \omega,$$

[1] In the field of view of the experiment.

where the subscript ℓ was used for the primary flux, but tag for the selected events. In fact, not all events tagged as light will be such and there will be a contamination from non-light (non$-\ell$) primaries. $c_{tag}(\mathbf{x},t)$ is the effective area for contaminating events. In the following, we assume that the contamination is well under econtrol, i.e. $c_{tag} \ll a_{tag}$, and its contribution is negligible. Also for light-tagged events it holds $a_{tag}(\mathbf{x},t) = g_{tag}(\mathbf{x})\, r_{tag}(t)$ and the ratio of event rates will be:

$$q_{tag}(\mathbf{x},t) = \frac{F_{tag}(\mathbf{x},t)}{F(\mathbf{x},t)} = \frac{\phi_\ell\,(\mathbf{x},t)}{\phi\,(\mathbf{x},t)}\,\frac{a_{tag}(\mathbf{x},t)}{a(\mathbf{x},t)} = \eta_\ell\,(\mathbf{x},t)\;\gamma_{tag}(\mathbf{x})\,\rho_{tag}(t),$$

where $\eta_\ell(\xi)$ is the ratio of primary fluxes and $\gamma_{tag}(\mathbf{x})\,\rho_{tag}(t)$ the ratio of the effective areas, separated in direction and time. We assume that the anisotropy of light primaries relative to the all-particle primary distributions is small, i.e.

$$\eta_\ell(\xi) = f_\ell\;(1+\delta_\ell(\xi))$$

where f_ℓ is the average fraction of light primaries selected by the applied tag and $\delta_\ell(\xi) \ll 1$.

2.2 The ratio-method

The relation between the observable $q_{tag}(\mathbf{x},t)$ and the ratio of primary fluxes $\eta_\ell(\xi)$ is deduced in the following. Let us consider the observable:

$$Q_{tag}(\xi) = \frac{\int_P \mathrm{d}t \int_{FOV} \mathrm{d}^2x\; q_{tag}(\mathbf{x},t)\,\frac{1}{\widetilde{\gamma}_{tag}(\mathbf{x})}\,\frac{1}{\widetilde{\rho}_{tag}(t)}\,w(\xi;\mathbf{x},t)}{\int_P \mathrm{d}t \int_{FOV} \mathrm{d}^2x\, w(\xi;\mathbf{x},t)}$$

where $w(\xi;\mathbf{x},t)$ selects only local coordinates corresponding to ξ, i.e. it is 1 if $\mathbf{x} = R(t)\xi$ and 0 otherwise. $\widetilde{\gamma}_{tag}(\mathbf{x})$ and $\widetilde{\rho}_{tag}(t)$ are observable estimators of $\gamma(\mathbf{x})$ and $\rho(t)$, for which it must be experimentally established the validity of the assumptions:

$$\widetilde{\gamma}_{tag}(\mathbf{x}) = \frac{\int_P \mathrm{d}t\, q(\mathbf{x},t)}{\int_P \mathrm{d}t} \leftarrow \gamma_{tag}(\mathbf{x})\, f_\ell\, \langle\rho_{tag}\rangle_P \left(1+\delta_\ell^{DEC(\mathbf{x})}\right)$$

$$\widetilde{\rho}_{tag}(\tau) = \frac{\int_{FOV} \mathrm{d}^2x \int_{P_\tau} \mathrm{d}t\, q(\mathbf{x},t)}{\int_{FOV} \mathrm{d}^2x \int_{P_\tau} \mathrm{d}t} \leftarrow f_\ell\,\rho_{tag}(\tau)\,(\langle\gamma_{tag}\rangle_{FOV} + \langle\gamma_{tag}\rangle_{DEC,FOV})$$

where P is the time-domain of the observation and FOV indicates the field of view. The symbol $\delta_\ell^{DEC(\mathbf{x})}$ indicates the average of $\delta_\ell(\xi)$ along the declination of the coordinate $\mathbf{x}$, whereas $\langle\gamma_{tag}\rangle_{DEC,FOV}$ indicates the average of γ_{tag} weighted with $\delta_\ell^{DEC(\mathbf{x})}$ and computed on the FOV. It is easy to demonstrate that

$$Q_{tag}(\xi) = \frac{1}{f_\ell^2\,(\langle\gamma_{tag}\rangle_{FOV} + \langle\gamma_{tag}\rangle_{DEC,FOV})\,\langle\rho_{tag}\rangle_P}\;\frac{\eta_\ell(\xi)}{1+\delta_\ell^{DEC(\xi)}},$$

which leads after normalisation to

$$\frac{\eta_\ell(\xi)}{1+\delta_\ell^{DEC(\xi)}} = f_\ell\,\frac{Q_{tag}(\xi)}{\langle Q_{tag}\rangle_{SKY}}. \tag{2.1}$$

where SKY is the portion of the sky in equatorial coordinates explored by the experiment. The equation (2.1) summarises the ratio-method: the ratio $Q_{tag}(\xi)$, suitably normalised, represents the

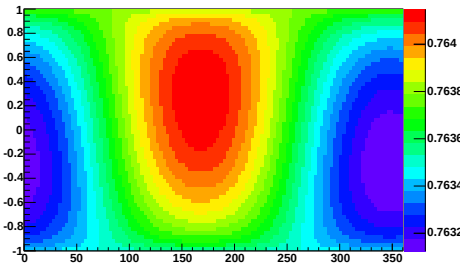

Figure 1: Ratio of light to all primary integral flux η_ℓ.

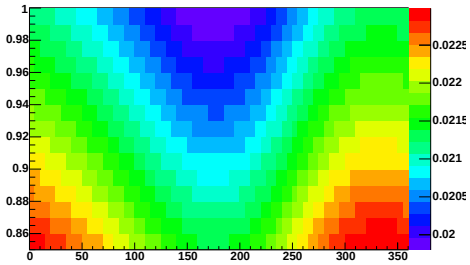

Figure 2: Ratio of (ϕ,θ)-dependent factors of effective areas γ_{tag}.

ratio of light primaries to all particles $\eta_\ell(\xi)$. Since these quantities are computed as a function of $\xi = (\alpha, \sin\delta)$, they can be mapped to represent how they are distributed in the sky, showing possible deviations from isotropy. Concerning the normalisation, we notice that f_ℓ does not depend on ξ and is an external parameter (coming from literature or independent measurements). The factor $1+\delta_\ell^{DEC(\xi)}$ instead shows that the measurement is not sensitive to amplitude variations along the declination, a feature common to all analysis methods to detect cosmic ray anisotropy with ground-based experiments.

3. Numerical simulations

We present here the result of numerical simulations performed to assess the validity of the ratio-method. The application to the full statistics of data will be presented at the conference and this text suitably modified.

3.1 Primary fluxes

To avoid any bias, we generated an all-particle distribution over the sky, with average integral flux of 11×10^{-3} m^{-2} sr^{-1} s^{-1} and dipolar anisotropy as intense as 10^{-3}. The dipole direction was randomly set to $(\alpha_{dip},\delta_{dip}) = (137^\circ,-27^\circ)$. In the same way, a light particle distribution was generated (8.4×10^{-3} m^{-2} sr^{-1} s^{-1} average integral flux, 1.5×10^{-3} dipolar anisotropy $(\alpha_{dip},\delta_{dip}) = (150^\circ,-10^\circ)$).

The ratio η_ℓ of these distributions is reported in figure 1. It represents the anisotropy of light elements *relative* to all particles. The average value is $8.4/11$ and a dipolar anisotropy as large as $\sim 0.9\times10^{-3}$ is visible.

3.2 Experimental setup

To reproduce all relevant features of ARGO-YBJ, a fast simulation was setup for an experiment placed at latitude $30^\circ N$, with field of view $FOV = \{(\phi,\theta)|\phi\in[0,360^\circ),\,\theta\in[0,30^\circ]\}$. The dependence of effective areas on ϕ and θ was set to be of the form:

$$g(\theta,\phi) = g_0\left[1+a_1\sin(\phi+\phi_1)+a_2\sin(\phi+\phi_2)\right](\cos\theta)^n.$$

	g_0	a_1	ϕ_1	a_2	ϕ_2	N
ALL	2200	0.008	0.0	0.004	25.7	5.5
LIGHT	44.5	0.035	90	0	0	5

Table 1: Effective areas used for the fast simulation.

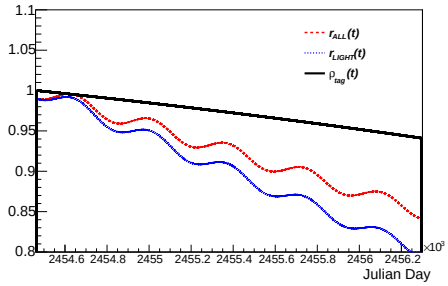

Figure 3: Time-dependent factors of effective areas r_{ALL} and r_{LIGHT} and their ratio ρ_{tag}.

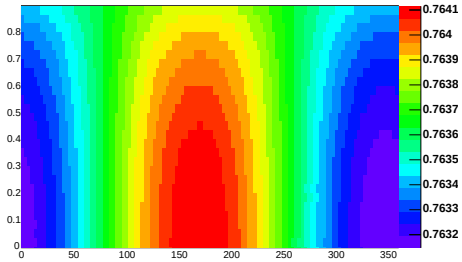

Figure 4: Right-hand member of equation 2.1 as computed in the numerical simulation.

Values of parameters for ALL and LIGHT selections are reported in table 1. Their ratio, named γ_{tag} to be consistent with notation of section 2, is reported in figure 2.

Data taking was simulated in the period 2008-2012. The dependence on time of effective areas was set to contain a seasonal variation and a weak loss of efficiency linear in time, of the form:

$$r(t) = r_0\,[1-\varepsilon\,(t-t_0)]\,[1+a\sin(\omega t)]\,.$$

t_0 coincides with the starting time of data acquisition, $\omega = 2\pi/(\mathrm{yr}/4)$ and the amplitude of the seasonal variance is set to be 10^{-2} for both LIGHT and ALL. The inefficiency ε was set to $3\times 10^{-2}\,\mathrm{yr}^{-1}$ for ALL and to $4\times 10^{-2}\,\mathrm{yr}^{-1}$ for LIGHT. The factors r_{ALL} and r_{LIGHT} are represented in figure 3, together with their ratio, named ρ_{tag} to be consistent with notation of section 2.

3.3 Closure tests

Input primary fluxes and effective areas described above were used to verify the validity of the ratio-method, i.e to verify to what extent the assumptions on $\widehat{\rho}_{tag}(t)$ and $\widehat{\gamma}_{tag}(\mathbf{x})$ hold. We observed systematic artefacts at the level 10^{-5}.

The right-hand side member of the equation (2.1) was computed and reported in figure 4. It looks slightly different from the input pattern visible in figure 1, but one should keep in mind that in the left-hand member of equation (2.1) does not appear η_ℓ alone, but corrected for the declination average.

To quantify the systematic bias introduced by the ratio method in estimating η_ℓ, the difference of right and left-hand member of equation (2.1) in units of the left-hand member was finally computed. This systematics turns out to be less than 1.5×10^{-5} everywhere in the sky under observation.

4. Conclusions

The measurement of the anisotropy for different primary particle masses in the knee energy region should be a high priority of the next generation ground-based experiments to discriminate between different propagation models of CRs in the Galaxy. A preliminary analysis of the CR anisotropy for (p+He)-induced events has been carried out with the ARGO-YBJ experiment. The analysis strategy is described in this paper. Results will be presented at the Conference.

References

[1] Di Sciascio G. and Iuppa R., On the observation of the Cosmic Ray Anisotropy below 10^{15} eV, in "Homage to the Discovery of Cosmic Rays, the Meson-Muons and Solar Cosmic Rays", Chapter 9, pagg. 221-257 (Nova Science Publishers, Inc., New York, 2013). Preprint: arXiv:1407.2144.

[2] Compton A.H. and Getting I.A., Phys. Rev., 47, 817, 1935.

[3] Abbasi R. et al., ApJ, 746, 33, 2012.

[4] Aglietta M. et al., ApJ Lett., 692, L130, 2009.

[5] Aartsen et al., ApJ, 765, 55, 2013.

[6] Desiati P. et al., NIM A, 742, 199, 2014.